Measurements of the Trace Composition of the Austral Stratosphere: Chemical and Meteorological Data

I. E. Galbally *et al.*

DIVISION OF ATMOSPHERIC RESEARCH TECHNICAL PAPER No. 1
COMMONWEALTH SCIENTIFIC AND INDUSTRIAL RESEARCH ORGANIZATION, AUSTRALIA 1983

Measurements of the Trace Composition of the Austral Stratosphere: Chemical and Meteorological Data

By I. E. Galbally, C. R. Roy, R. S. O'Brien, B. A. Ridley, D. R. Hastie, W. F. J. Evans, C. T. McElroy, J. B. Kerr, P. Hyson, W. Knight and J. E. Laby

Division of Atmospheric Research Technical Paper No. 1

Commonwealth Scientific and Industrial Research Organization, Australia

1983

TABLE OF CONTENTS

CSIRO Aust. Div. Atmos. Res. Tech. Pap. No. 1, 1-31 (1983)

Measurements of the Trace Composition of the Austral Stratosphere: Chemical and Meteorological Data

I.E. Galbally[1], C.R. Roy[1*], R.S. O'Brien[1*], B.A. Ridley[2], D.R. Hastie[2], W.F.J. Evans[3], C.T. McElroy[3], J.B. Kerr[3], P. Hyson[1], W. Knight[1] and J.E. Laby[4]

1. CSIRO, Division of Atmospheric Research, Aspendale, Victoria, Australia
2. Department of Chemistry, York University, Downsview, Ontario, Canada
3. Atmospheric Environment Service, Department of the Environment, Downsview, Ontario, Canada
4. School of Physics, Royal Australian Air Force Academy, University of Melbourne, Australia

* now at the Australian Radiation Laboratory, Department of Health, Yallambie, Victoria, Australia

ABSTRACT

Between March and October 1979 eleven balloon flights were conducted to study the trace composition of the southern hemisphere stratosphere using launch sites at Alice Springs 23°S and Mildura 34°S in Australia. Balloon borne measurements of NO, NO_2, HNO_3, O_3, N_2O, CCl_3F, H_2O, CH_4, particles (> 0·15 μ and >0·25 μ radius) and various meteorological parameters along with ground based total (column density) O_3 and NO_2 measurements are presented in this report.

This work was performed under Memorandum of Understanding AIA/CA-17 between the Federal Aviation Administration, Department of Transportation, United States of America and the Commonwealth Scientific and Industrial Research Organization, Australia.

1. Introduction

The purpose of these measurements was to obtain a comprehensive set of data of nitrogen compounds and other trace gases in the southern hemisphere stratosphere for validation of theoretical models of the composition and chemistry of the stratosphere, for use as part of the ground truth plan for the Stratospheric Aerosol and Gas Experiment SAGE on the AEM-B (NASA) satellite, and to remedy the lack of data on nitrogen compounds and other trace gases in the southern hemisphere stratosphere.

The measurements were carried out in autumn and spring, these being the time of minima and maxima in stratospheric ozone over Australia (Pittock 1977a). The balloon launchings were conducted from Alice Springs 23°20'S, 134°0'E, 545 m.a.s.l., and Mildura 34°13'S, 142°12'E, 53 m.a.s.l.

Two different balloon borne sets of measuring equipment were used for eleven flights in 1979. These were:

(1) a "large" gondola containing equipment measuring NO, NO_2, HNO_3, O_3, standard radiosonde parameters and, on the last two flights, particles flown with a 42,500 or 57,000 m^3 balloon, and

(2) a "small" gondola holding the grab sample spheres for collecting stratospheric air samples along with O_3 and H_2O instruments and standard radiosonde equipment flown with a 8500 m^3 balloon.

In 1977 there were two other flights on which the NO instrument was flown alone (Roy, Galbally and Ridley, 1980). This data is included here for completeness.

Each balloon was tracked by a nearby Australian Bureau of Meteorology standard balloon tracking radar (type WF2 or WF44) and this data was analysed to deduce values of balloon height, balloon position, wind speed and direction as functions of time from launch.

The large gondola also carried a Rosemount pressure sensor to measure altitude and radio ranging equipment for location. In some cases these measurements were used to supplement the radar data.

Analyses of these data were conducted by standard methods described in the Appendix.

Some additional ozonesonde/radiosonde flights were made using standard meteorological type balloons.

Flask samples for N_2O and CCl_3F were taken in the lower troposphere from light aircraft on several occasions to complement the balloon borne stratospheric grab sampling.

Total (column density) ozone measurements were made from the ground throughout each field expedition. Also ground based total (column density) NO_2 measurements were made on suitable occasions.

The data obtained on the different flights is summarised in Table 1.

TABLE 1

DATA AVAILABLE FOR STRATOSPHERIC BALLOON FLIGHTS

DATA AVAILABILITY Y = YES
N = NO

LAUNCH SITES AS = ALICE SPRINGS
ML = MILDURA

FLIGHT CODE	DATE	LAUNCH TIME (UT)	LAUNCH SITE	RADAR TRACKING	NO	NO_2	HNO_3	O_3	N_2O $CFCl_3$	CH_4	H_2O	AEROSOL
ABLS688	771211	195700	ML	Y	Y	N	N	N	N	N	N	N
ABLS690	771213	195900	ML	Y	Y	N	N	N	N	N	N	N
ABLS714	790323	205700	AS	Y	N	N	N	Y	Y	N	Y	N
OZAS001	790325	011500	AS	N	N	N	N	Y	N	N	N	N
ABLS715	790328	213000	AS	Y	Y	N	Y	N	N	N	N	N
ABLS716	790403	214500	AS	Y	N	N	N	Y	Y	N	Y	N
ABLS719	790409	174500	AS	Y	Y	N	Y	Y	N	N	N	N
ABLS722	790509	212300	ML	Y	N	N	N	Y	Y	N	Y	N
ABLS723	790515	174400	ML	Y	Y	N	Y	Y	N	N	N	N
ABLS724	790517	220000	ML	Y	N	N	N	N	Y	N	Y	N
ABLS735	790918	205600	ML	Y	N	N	N	N	Y	Y	Y	N
OZML001	791004	035600	ML	N	N	N	N	Y	N	N	N	N
ABLS736	791013	210900	ML	Y	N	N	N	N	N	N	Y	N
ABLS737	791015	171900	ML	Y	N	Y	Y	N	N	N	N	Y
OZML002	791016	012000	ML	Y	N	N	N	Y	N	N	N	N
OZML003	791020	011600	ML	Y	N	N	N	Y	N	N	N	N
OZML004	791024	052200	ML	Y	N	N	N	Y	N	N	N	N
ABLS738	791025	050600	ML	Y	Y	Y	Y	Y	N	N	N	Y
OZML005	791026	032330	ML	N	N	N	N	Y	N	N	N	N

2. MEASUREMENT TECHNIQUES

2.1 Nitric Oxide (NO)

The chemiluminescent technique for measuring NO is well known. It is based on detecting the intensity of the radiation emitted by excited NO_2 molecules following the reaction $NO + O_3 \rightarrow NO_2 + O_2$ when an excess of O_3 is added to a flow of air containing NO. The emitted radiation is a continuum with its maximum intensity occurring near 1200 nm. As such the detection method is not entirely specific, in that other atmospheric constituents which undergo chemiluminescent reactions with O_3 in the spectral region viewed by the instrument will contribute to the NO signal. Other gases such as unsaturated hydrocarbons are known to chemiluminesce with O_3 but with much lower efficiency than that of NO in this spectral region. Since these gases are not expected to be present in the stratosphere in concentrations as high as those of NO, it is unlikely that such interference will be significant, although to be strictly rigorous, the present technique must be viewed as providing an upper limit to the NO density.

The balloon instrument used is described in Ridley et al. (1975) and Ridley (1978). The weight and size of the instrument without the O_3 supply and inlet and exhaust tubes are about 45 kg and 0.4 by 0.4 by 0.25 m, respectively. The reaction vessel is a Pyrex cylinder with a reflective gold coating. A PMT cooled by dry ice views the length of the tube through a filter that transmits wavelengths above about 600 nm. The PMT is insensitive to wavelengths above about 900 nm. Therefore, only a small fraction of the continuous emission may be sampled.

Ambient air is drawn through a 2 m length of pyrex glass tube. After being heated to approx. 300°K and mixed with O_3 in the reaction vessel and the light emission measured, the air is exhausted through a 10 cm diameter tubing at least 2 m in length attached upwards to the support cables.

As high an airflow as possible is desired, therefore, the instrument pressure drop is kept low by the use of large-diameter tubing throughout. The need for light baffles to exclude sunlight is obvious. Proportional controlled heaters raise the ambient gas temperature to about 300 K. Ambient air is drawn through the instrument by a squirrel-cage fan that is approximately a constant volume pump. Below an altitude of about 22 km a flow controller limits the total airflow to about 275 sccs. Near an altitude of 28 km the pumping efficiency drops to about 100 sccs. The airflow, pressure, and temperature are measured in the inlet section by appropriate calibrated transducers.

At present, O_3 is stored and flown in stainless steel or aluminium cylinders as a solution of 6-10% O_3 in CF_3Cl at the temperature of dry ice. The vaporized flow of this mixture to the instrument is controlled at about 10 sccs. This O_3/CF_3Cl mixture was prepared in Australia prior to the flights.

The instrument cycles through three modes by timer control of stainless steel solenoid valves. In the first, zero mode, ozone is added through a valve well upstream of the reaction vessel. The purge volume of the instrument is about six times larger than that of the reaction vessel, and the residence time for the O_3 flow used is sufficient to remove ambient NO from the air sample prior to its reaching the reaction vessel. At the same time, the change in the O_3 concentration is negligible; recorded counts are due to the background O_3 emission. In the measure mode, O_3 is added by way of a valve 2 through a

mixing flange at the PMT end of the reaction vessel. Thus, the difference in signal counts between these two operational modes is proportional to the ambient NO mixing ratio. The instrument is calibrated between every purge and measure mode by adding known amounts of NO from a high-pressure tank containing a few ppm (volume) of NO in N_2 through the inlet tube while in the measured mode. The difference in counts between the inlet tube calibration and measure modes is thus attributable to the addition of the known NO flow.

The calibration tanks are evacuated to low pressure with a diffusion pump and filled from a larger gas cylinder whose mixing ratio is checked periodically by the supplier, is cross-checked with a standard from another supplier, and is checked periodically with the use of a mass spectrometer. At present the flight tanks are analysed against the standard before and after each flight. The error in the mixing ratio determined in this way is usually less than ±15%. Any error is directly transferred to the stratospheric measurement.

The accuracy of the measurement is determined by errors in the calibration gas analysis, the airflow measurement (±7%), and the calibration gas flows (±4%) if the ambient NO concentration is not perturbed by the measurement technique.

The nitric oxide data is collected as measurements over a short time interval (∿8 sec). This data is regularly interrupted by a zero and calibration sequence and this accounts for the regular gaps in the data between extended periods of regular data gathering. During some flights, signal averaging over longer periods has been used to reduce noise in the data.

2.2 Nitrogen Dioxide (NO_2)

Gaseous nitrogen dioxide has a spectrum which is strongly structured in the region 430 to 450 nm. (Johnson et al 1976, Hall et al 1952). The rapid variations in the absorption coefficient permit the application of differential spectrophotometry to the measurement of NO_2 in the Earth's atmosphere. The differential absorption coefficient is sufficiently large that the technique is sensitive to the small quantities of NO_2 that are found in the atmosphere.

The Fraunhofer structure of the solar spectrum, the presence of stratospheric ozone in the atmosphere and the effects of particulate and Rayleigh scattering make the measurement of NO_2 difficult. The application of differential spectrophotometry to the problem overcomes these difficulties and allows the dependable determination of the column amount and vertical distribution of this important stratospheric constituent.

If one considers the transit of a ray of light through the atmosphere from a distant source (usually the sun) to the instrument, where its spectral intensity is measured; the intensity of light at some wavelength λ_i may be written as (Beer's law):

$$I(\lambda_i) = I_o(\lambda_i)\ 10^{-(\alpha_i X + \beta_i M + \delta_i q + \gamma_i Y)\mu} \qquad (1)$$

Where the symbols used are:-

α_i - absorption coefficient at λ_i for ozone (cm^{-1})

β_i - Rayleigh scattering coefficient (atm^{-1})

δ_i - coefficient for attenuation by particulate scattering and absorption (cm^{-1})

γ_i - absorption coefficient at λ_i for NO_2 (cm^{-1})

X - column amount of ozone (atm-cm)

M - total amount of air in column (atm)

q - column amount of haze (atm-cm)

Y - total amount of NO_2 (atm-cm)

μ - geometric amplification factor of the vertical column amounts

(For the path length to a specific point, μ is the Chapman function $Ch(X,\chi)$ and reduces to sec χ for high sun angles).

This relation, by virtue of the use of the common factor μ to represent the geometrical amplification of absorption, assumes that the absorbers are all distributed with the same vertical and lateral variations, so that the common factor μ may be extracted.

In practice, the intensity at various wavelengths is measured and this information is used to calculate the amount of some absorber. The equation (1) may be rewritten as:

$$\log(I_i) - \log(I_{oi}) = [-\alpha_i X - \beta_i M - \delta_{ig} - \gamma_i Y]\mu \qquad (2)$$

The constant $\log(I_{oi})$ is the extraterrestrial intensity of the source. This is the intensity that the instrument would measure if no absorption were taking place in the incident path. It is the value which would be measured if $\mu = 0$ in the equation (2).

Traditionally, in direct sun observations, the value $\log(I_i)$ in equation (2) was plotted as a function of μ to derive the intercept, which was interpreted as the extraterrestrial constant.

If measurements at a number of wavelengths are made, a linear combination of their logarithms may be created. For example:

$$F = \sum_{i=1}^{N} a_i \log(I_i) \qquad (3)$$

where F, the absorption function is sensitive to the absorption of some species in the atmosphere and the a_i are the weighting constants.

From equation (2) we may write:

$$\frac{F-F_o}{\mu} = -X \sum_{i=1}^{N} a_i\alpha_i - M \sum_{i=1}^{N} a_i\beta_i - q \sum_{i=1}^{N} a_i\delta_i - Y \sum_{i=1}^{N} a_i\gamma_i \qquad (4)$$

Furthermore, we can require that the instrument be insensitive to the absolute intensity of the source and the absolute sensitivity of the spectrophotometer. This means that the derivation of absorption amounts is based only on the relative absorptions between different wavelengths.

The condition of no absolute sensitivity may be written as follows:

$$I_i = K_i I$$

where K_i - relative intensity between wavelengths. Arbitrarily any K_i could be one, and the rest set accordingly.

I - represents the absolute intensity as measured by the instrument at some wavelength λ.

The independence of the function from intensity variations requires that I drop out of the equation for F.

$$F = \sum_{i=1}^{N} a_i \log(K_i I) \qquad (5)$$

$$= \sum_{i=1}^{N} a_i \log K_i + \sum_{i=1}^{N} a_i \log I$$

The second term, in I, will disappear only if:

$$\sum_{i=1}^{N} a_i \equiv 0 \qquad (6)$$

The maintenance of stable relative sensitivity is itself difficult if high accuracy is required. This is so because the structure of the solar spectrum translates any wavelength shifts into large intensity changes. The requirement on wavelength stability may be reduced, however, if the various wavelengths measured are combined in such a way that a shift of the calibration point, which affects all wavelengths, causes cancelling changes on different wavelengths. The requirement may be expressed mathematically as

$$\frac{dF}{d\lambda} \equiv 0 \qquad (7)$$

while observing the sky or solar spectrum. Any change associated with a small displacement in calibration $\delta\lambda$ will then show a minimal effect on the absorption function F.

This equation translates to:

$$\sum_{i=1}^{N} a_i \frac{d}{d\lambda} (\log I_i) \equiv 0 \qquad (8)$$

In practice, the lack of information concerning the characteristics of haze (δ_i, q) have led to their neglect. This is not a serious omission as will be seen later.

The final absorption function should meet the following criteria:

a) $\Sigma a_i = 0$ - independence from absolute sensitivity and intensity.

b) $\Sigma \alpha_i a_i = 0$ - no response to atmospheric ozone.

c) $\Sigma \beta_i a_i = 0$ - no response to Rayleigh scattering.

d) $\Sigma a_i \frac{d}{d\lambda}(\log I_i) = 0$ - small sensitivity to small errors in wavelength calibration.

e) $\Sigma a_i \gamma_i = 1$ - unit sensitivity to NO_2.

The operational wavelengths for the measurement of NO_2 are 437.6 nm, 439.3 nm, 442.0 nm, 444.9 nm and 450.1 nm, with slit widths equivalent to approximately 0.4 nm. The absorption coefficients for these wavelengths are taken from Johnson et al. (1976) and are smoothed to the appropriate resolution. They are assumed to be independent of temperature (Bass et al, 1976). The pressure dependence of the NO_2 absorption cross section has been investigated, and the effect was found to be negligibly small in this application. The value of the coefficients appropriate for the measurements of NO_2 are:

$$a_1 = 0.126$$
$$a_2 = -0.161$$
$$a_3 = 0.122$$
$$a_4 = -0.162$$
$$a_5 = 0.075$$

For this choice of coefficients Rayleigh scattering is completely suppressed. Since it has a wavelength dependence of λ^{-4}, we expect that any interference from particulate scattering will be small over this wavelength range.

During the program of balloon flights in Australia, two types of measurements were made. One type was a solar occultation measurement from the balloon platform, and the other was a ground based method using light scattered from the zenith sky. Unfortunately, instrumental problems with the solar tracking system on the NO_2 spectrometer permitted the acquisition of data during the October flights only (sunrise October 16 and sunset October 25). However, an extensive program of ground based measurements was undertaken and these provide ground-based NO_2 data for the earlier flights.

In both measurement techniques the same instrument was used. For observations of the sky a 10 cm focal length f/5 lens images the sky on the entrance slit of the spectrometer. The solar pointing observations are made with a diffuser made of ground glass, which is kept illuminated by a motorized prism pointing system.

The spectrophotometer has been described elsewhere by Brewer (1973) and Kerr et al (1976). It is a 15 cm focal length Ebert design, which images a spectrum dispersed by a Bausch and Lomb 1200 line per millimeter replica grating onto a focal plane, where a chopper system operated by a microcomputer-controlled stepper motor sequentially samples light from each of the five operational wavelengths. The light is collected by a Fabry lens which images the grating surface on the photocathode of a low noise photomultiplier. The discriminated photon count pulses are accumulated by the microprocessor which relays the results via telemetry, or a hard wired connection, to a recording terminal or processing computer.

The instrument control computer also operates the solar pointing system which is capable of acquiring, as well as tracking the sun.

2.2.1 Balloon-borne Measurements

The method of solar occultation measurements has been extensively reported in the literature, and will not be considered in detail here, (Chapman, 1931, Kerr et al, 1977). Suffice it to say that for an incident ray as shown in Figure 1, the majority of the absorption experienced by the light will occur in the region near the tangent height. Many analytical expressions and approximations have been developed for this case, but the simplifying assumptions embodied in them preclude their use in accurate profile determinations. (See Smith et al, 1973 for approximations to the Chapman function under various circumstances). In addition, the effects of refraction must be allowed for. Because of the changing mixing ratio with height of NO_2 in the stratosphere and because of the vertical temperature structure, the analysis method used to extract the NO_2 profile is a layer by layer approach, developed by one of us (J.B. Kerr). The figure demonstrates the principle. The first layer below the balloon height is calculated using the difference in the instrument's absorption function between angles just before and just after a solar zenith angle of 90°. The amount of NO_2 calculated to be in this layer is then used to make a correction for the part of the next lower tangent ray's passage through the top layer. This process is then applied to layers corresponding to angles farther removed from 90°.

The effect of refraction is included in this analysis by allowing the rays to change direction in crossing between layers in accordance with Snell's Law, and the vertical density gradient of the atmosphere. The point conjugate to the instrument position on the opposite side of 90° solar zenith angle is the one which corresponds to the same refracted ray.

There is a correction to the profile which is required if the reported profile is to reflect accurately the amount of NO_2 in the stratosphere at 90° solar zenith angle. The amount of NO_2 in any layer changes with time due to the shift in photochemical equilibrium between NO and NO_2. As the sun sets or rises the photodissociation rate for NO_2, J_{NO_2} changes and this causes the amount of NO_2 in any layer to alter due to the reaction:

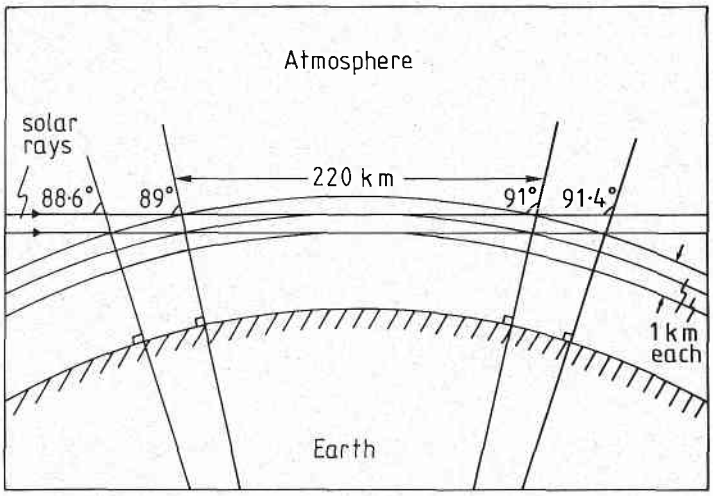

Figure 1. Geometry of the optical NO_2 measurement

$$NO_2 + h\nu \rightarrow NO + O \qquad \text{rate} = J_{NO_2} \qquad (9)$$

Therefore the correction applied to tangent heights well below the balloon height due to NO_2 higher up, will be in error because of the change in the amount of NO_2 in the layers above. This correction has been reported (Kerr et al, 1977) and amounts to a maximum of ∿20% at 22 km. The results reported here have not been corrected. A similar study for NO and C&O was done by Boughner et al (1980).

The uncorrected profiles slightly overestimate the amount of NO_2 at all levels between 14 and 28 km, over the true amount corresponding to 90° solar zenith angle at each layer.

The errors in the NO_2 mixing ratios were derived from the statistics of the photon counting method used to measure the scattered light intensity, and are presented with the derived values of NO_2 mixing ratio and molecular column amount for the various layer thicknesses in the data tables. The uncertainty in higher layers is reflected in the calculation of the errors for lower layers because of the iterative corrections in the inversion algorithm.

2.2.2 Ground Based Measurements

The technique used to make measurements of stratospheric nitrogen dioxide from the ground has also been reported in the literature (Brewer et al, 1973, 1974, Noxon et al, 1979, Seyd et al, 1980). In brief, the technique utilizes the tangent ray enhancement of absorption at high levels by observing the zenith sky with the spectrophotometer. As the sun sets (or rises) the long path absorption of the incoming solar radiation at

angles near or greater than 90°, is forced to occur at higher levels in the stratosphere because of the depletion of low level light by Rayleigh scattering. This has the effect that the later part of the absorption curve is influenced most by NO_2 at higher levels.

The amount of NO_2 in the atmosphere is estimated by comparing the response of a synthetic absorption curve from a multiple scattering model with NO_2 inserted in various layers, to that of the experimental data from the atmosphere. The model has been described by Dave et al. (1967) and Heath et al. (1973).

The application of this technique allows the separation of NO_2 which is very low in the atmosphere from that which is in the stratosphere (actually that NO_2 above 13.6 km). Therefore, an estimate of the stratospheric column amount can be made, in the presence of low level, tropospheric NO_2. The amounts reported here are uncertain by approximately 50%, and the effect of the night-day conversion of NO_2 to NO has not been directly calculated as yet. The inter-comparison of balloon measurements and ground measurements made during the same period provides confidence in the results of this method (see later table).

There are some missing entries in the table. It was impossible to derive any distributional information about the NO_2 amount on those days because the fit of the calculated curves to the observations was very poor. This was probably due to the temporal variation of tropospheric NO_2 during the sunrise period.

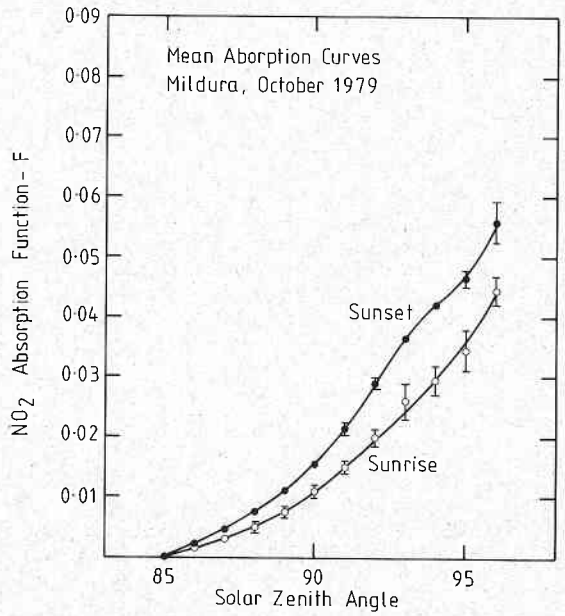

Figure 2. NO_2 absorption function for Mildura October 1979

The graph in Figure 2 is the data set for October 1979. The individual curves were normalized to the function value of 85°, and then the curves were averaged (Mateer, 1964). The error bars represent the standard deviation of the mean estimated for each curve. This procedure removes variations in the observed data due to low level NO_2, or due to small variations in the instrument extraterrestrial constant, F_o. Using this procedure, curves representative of October were constructed for both sunrise and sunset. These curves were then analysed to derive the NO_2 amounts reported in the following table, section 3.7.

2.3 Nitric Acid (HNO_3)

2.3.1 Method of Detection

The nitric acid radiometer has been described by Evans et al. (1976). The theory of this measurement is described below.

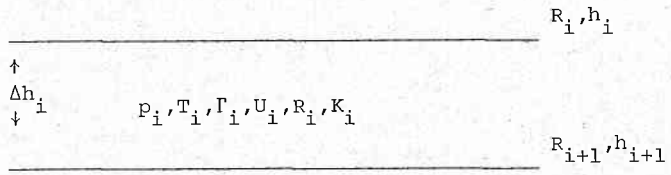

Notation:

Δh_i = thickness of layer i
ΔR_i = change in radiance across layer i
p_i = mean pressure of layer i
T_i = mean temperature of layer i
Γ_i = mean transmission of layer i
K_i = mean absorption coefficient for layer i
U_i = nitric acid column amount in layer i
B_i = mean black-body radiance in layer i

The equation of radiative transfer for a ray passing through layer i at an angle θ to the vertical is given for any wavenumber ν by

$$R_{i+1,\nu} = R_{i,\nu} + \Delta R_{i,\nu} = R_{i,\nu}\, T_{i,\nu} + B_{i,\nu}\,(1 - T_{i,\nu}) \qquad \ldots (1)$$

where

$$T_{i,\nu} = \exp\,(-K_{i,\nu}\, U_i \sec\theta) \qquad \ldots (2)$$

If we assume that $T_{i,\nu} \simeq 1$, $R_{i,\nu} \ll B_{i,\nu}$ and that $B_{i,\nu}$ varies slowly with wavenumber by comparison with $K_{i,\nu}$ then we can integrate (1) with respect to wavenumber to give the result

$$\Delta R_i = B_i\, U_i\, K_i \sec\theta \qquad \ldots (3)$$

The measurements of Goldman et al. (1981) indicate that $K_{i,\nu}$ does not vary significantly with temperature over the range of temperatures encountered in the stratosphere so we have taken K_i to be independent of temperature.

The absorption coefficient K_i is calculated from the formula

$$K_i = \frac{\int_{\Delta\nu} K_{i,\nu} F_\nu d\nu}{\int_{\Delta\nu} F_\nu d\nu} \qquad \ldots (4)$$

where F_ν is the measured filter transmission at wave-number ν, $\Delta\nu$ is the pass-band of the filter, and $K_{i,\nu}$ is the absorption coefficient of the 11.3 μm band, as given by Goldman et al. (1981).

Equation (3) can be used to calculate the mixing ratio U_i, as all the other quantities are known or can be measured during flight.

The value used for $\sec\theta$ was 3.2. This value was found by measuring the zenith angle of the axis of the radiometer, and then allowing for the field of view of the radiometer by integrating the path length over the finite angular aperture of the instrument.

It was assumed that the voltage output of the radiometer could be computed from the formula

$$V = G_V G_P (R_S - R_O) \qquad \ldots (5)$$

where

V = output voltage

G_V = voltage gain (pressure independent)

G_P = voltage gain (pressure dependent)

R_S = source radiance

R_O = chopper radiance (chopper assumed to be at 77 K)

The radiometer was calibrated in two ways. The pressure independent sensitivity (G_V) was measured using a source whose temperature could be varied to produce a range of radiance values similar to those encountered in the atmosphere. The variation of sensitivity with pressure (G_P) was measured using a high altitude simulation chamber and a constant temperature source.

The relative errors in the two calibration terms, as indicated by reproducibility of the calibrations (standard deviations of individual measurements) are ±15% in a radiance measurement and ±1.5% in the pressure correction.

The filter transmissions were measured using an infra-red spectrophotometer and a special filter holder which allowed the filter to be held in thermal contact with a reservoir of liquid nitrogen. The relative transmission of the filters (at liquid N_2 temperature) is shown in Figure 3.

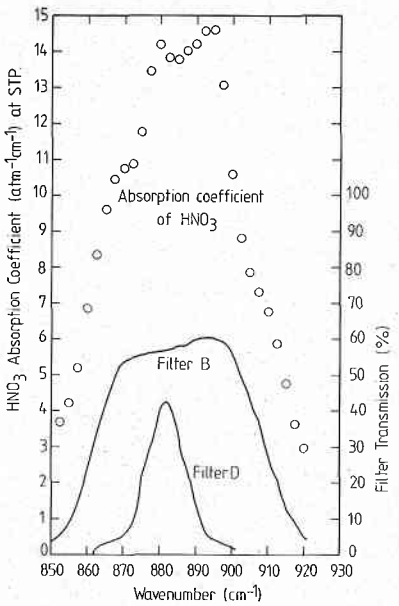

Figure 3. HNO_3 absorption coefficient and instrument filter transmission functions

2.3.2 Analysis of Flight Data

In flight, during balloon ascent and descent, the output voltage of the radiometer was measured for each filter as a function of time. The voltage/time data were then combined with the height/time data, the pressure/time data and the results of the laboratory calibrations to produce values of radiance versus height for each filter. The data from the two filters were then combined in the following way.

If the transmission curves of the two filters are centered on wavenumbers ν_B and ν_D respectively, then we define

$$\bar{\nu} = \frac{1}{2}(\nu_B + \nu_D) \qquad \ldots (6)$$

Using the measured values of ν_B and ν_D, it can be shown that, over the range of temperatures encountered in the stratosphere, the following relations hold to a very good approximation (within 2.5%)

$$\left.\begin{aligned} B_i(\nu_B) &= f_B B_i(\bar{\nu}) = f_B \bar{B}_i \\ B_i(\nu_D) &= f_D \bar{B}_i \end{aligned}\right\} \qquad \ldots (7)$$

when f_B and f_D are constant, $\bar{B}_i \equiv B_i(\bar{\nu})$, and $B_i(x)$ is the black-body radiance at wavenumber x. If we substitute this result in Equation (3) we have

$$\Delta R_i = K_i \; f \; \bar{B}_i \; U_i \; \sec\theta \qquad \ldots (8)$$

$$\text{or} \quad R_{J+1} = \sum_{i=1}^{J} f \; K_i \; \bar{B}_i \; U_i \; \sec\theta + R' \qquad \ldots (9)$$

where R' is the contribution from a source outside the atmosphere and it is implicitly assumed that radiation from this source is not absorbed within the atmosphere.

$$\text{Defining } R^* = R/(fK_i) = \text{normalized radiance} \qquad \ldots (10)$$

we see that the quantity R* is independent (to the degree of approximation assumed in equation (7)) of the filter, so the radiance/height profiles from each filter can be combined to form a single profile of R* versus height.

The R*/height data were smoothed using a least-squares cubic spline fitting method. The original data and the fitted curves are shown in Figures 4 to 8. The value of the fitted curve was taken at the boundary of each atmospheric layer and the change in R* across each layer was then calculated.

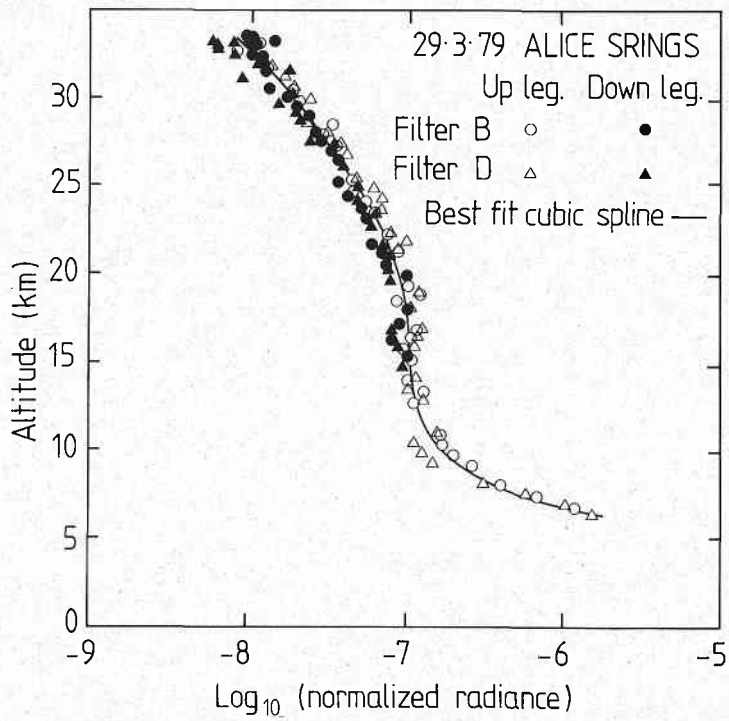

Figure 4 Normalized radiance - Altitude distribution for Alice Springs 29.3.1979, Radiance in $Wm^{-2}\ sr^{-1}\ \mu m^{-1}$

Equations (8) and (10) show that

$$\Delta R_i^* = \bar{B}_i U_i \sec \theta \qquad \ldots (11)$$

so the amount U_i (in atm.cm, at STP) can be calculated for each layer. This amount U_i is then converted to volume mixing ratio using the fact that the total number of nitric acid molecules in layer i ($\int_{\Delta h_i} ndh$) is related to U_i by

$$\int_{\Delta h_i} ndh = LU_i \qquad \ldots (12)$$

where L is Loschmidt's number (= 2.687×10^{25} mol. m^{-3} at STP) and n is the number density of nitric acid molecules at height h, while the total number of air molecules in layer i is given by (if N is the number density of air molecules at height h)

$$\int_{\Delta h_i} Ndh \simeq \frac{\Delta h_i}{2k} \left(\frac{P_i\,(\text{top})}{T_i\,(\text{top})} + \frac{P_i\,(\text{bottom})}{T_i\,(\text{bottom})} \right) \qquad \ldots (13)$$

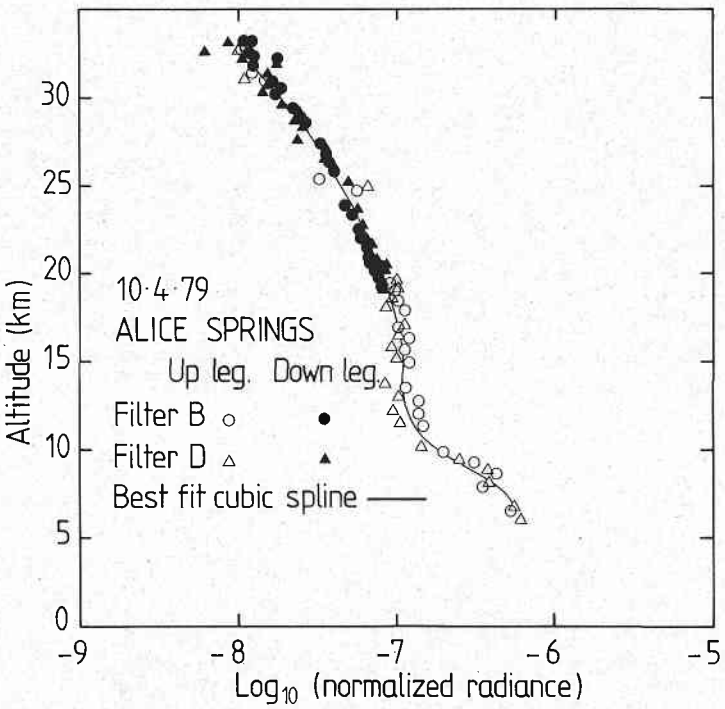

Figure 5 Normalized radiance - Altitude distribution for Alice Springs 10.4.1979, Radiance in $Wm^{-2}\ sr^{-1}\ \mu m^{-1}$

where k = Boltzmann's constant (= 1.3808 x 10^{-23} joule K^{-1}). The mixing ratio is then given by

$$Q_i = \frac{\int_{\Delta h_i} ndh}{\int_{\Delta h_i} Ndh} \qquad \ldots (14)$$

Analysis of the flight data shows that the scatter in the radiance values is ±15%, in keeping with the variations observed during the laboratory calibrations. Statistical theory predicts, given this scatter, the total change in radiance through the depth of the stratosphere sampled (∿15-32 km) and the number of radiance measurements made, that the information content from a flight profile allows independent values of nitric acid content for approximately twelve layers to be determined, each concentration having an r.m.s. error of 50%, or five layers to be determined, each concentration having a r.m.s. error of 25%.

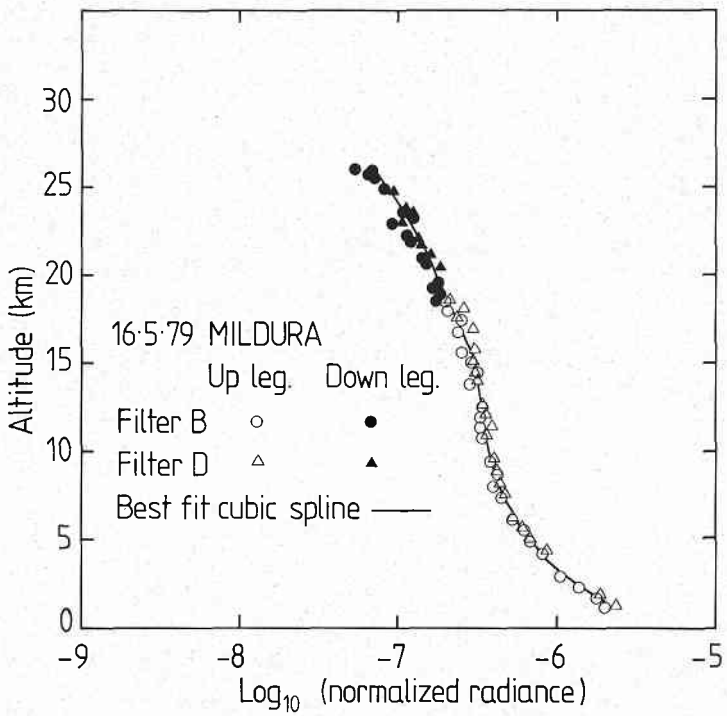

Figure 6 Normalized radiance - Altitude distribution for Mildura 16.5.1979, Radiance in Wm^{-2} sr^{-1} μm^{-1}

The major source of absolute error in this method comes from the nitric acid absorption coefficient and we have no estimate of this error.

The nitric acid data yielded from the data processing are 1 km averages and therefore no detailed data apart from the radiance/height figures are presented. For flights ABLS, 715, 719, 723, 737 both ascent and descent data are used to derive the HNO_3 profiles. On flight ABLS 738 there was a systematic shift in the radiance profile between ascent and descent which could be caused by either a change in HNO_3 above the balloon altitude or a shift in the calibration of the measurement system. Due to this systematic difference the data for the ascent only were used to derive the HNO_3 profile. Note the descent radiance profile would give approximately the same HNO_3 concentration profile in the height range traversed as the measurement of HNO_3 is dependent on the rate of change of radiance with altitude, not the absolute value.

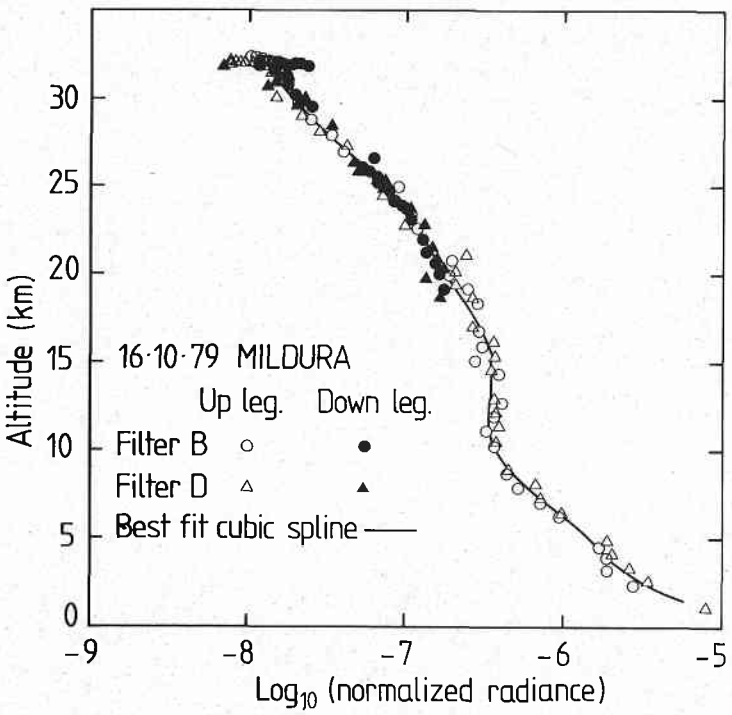

Figure 7 Normalized radiance - Altitude distribution for Mildura 16.10.1979, Radiance in $Wm^{-2}\ sr^{-1}\ \mu m^{-1}$

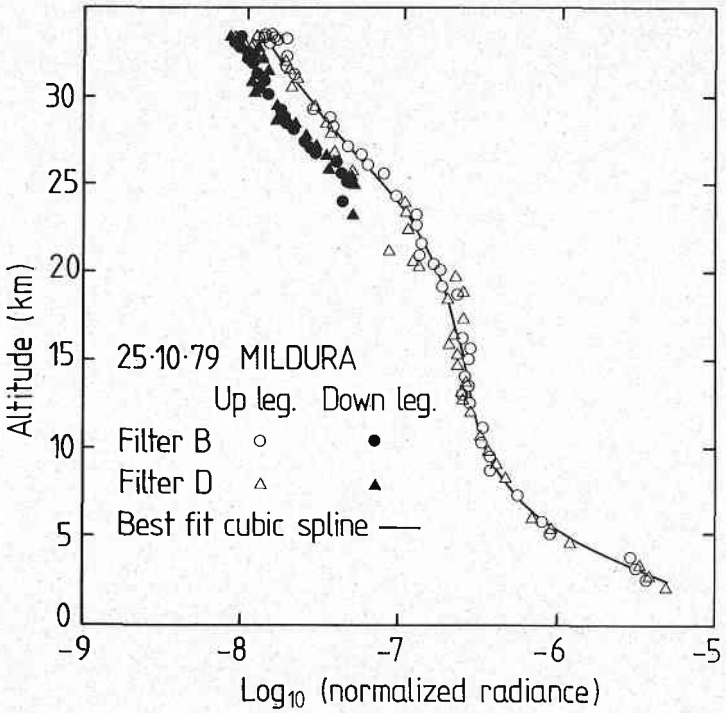

Figure 8 Normalized radiance - Altitude distribution for Mildura 25.10.1979, Radiance in Wm^{-2} sr^{-1} μm^{-1}

2.4 Ozone

Total (ground based) ozone measurements were made with Dobson instrument No. 111. This instrument was intercalibrated with the WMO Region V standard instrument No. 105 at Aspendale. Regular mercury lamp (wavelength) standard lamp (sensitivity) and L_o (extraterrestrial constant) tests were performed during the field measurements and the data was reduced by the standard methods.

Mast-Brewer Model 730-6 ozone sondes were used to obtain the vertical ozone distributions. Standard preparation and calibration procedures were used for these ozone sondes. Some difficulties were encountered on early flights due to contamination of the bubblers by the exhaust gases from the launch vehicle. (This is normally not a problem when meteorological balloons are used as the latter are hand-launched.) On later flights pressure switches were fitted so that the bubbler pump commenced working only after the balloon was above ∿900 mb. The ozone profiles measured by the ozone sondes were corrected to the total ozone amount measured by the Dobson spectrophotometer using the Dütsch method as discussed by Pittock (1977b).

The errors in the derived values of ozone from the sonde instruments are assumed to be of the order of ±9%, made of up ±5% due to pump corrections and ±7% due to random errors (Hudson and Reed, 1979).

As discussed in the data analysis appendix some of the flights do not have radar tracking for altitude. On these flights the height is derived from the pressure and temperature data. This is indicated on the data heading. The ozone data is presented in two units, the partial pressure of ozone as nb $\equiv 10^{-9}$ bar and as mixing ratio.

2.5 Grab Samples

2.5.1 The Sampling System

The grab sample system was originally built at the NOAA laboratory in Boulder and has been briefly described by Schmeltekopf et al. (1975).

A sample sphere is shown schematically in Figure 9. The grab sample system consists of five evacuated spheres and their associated electronics,

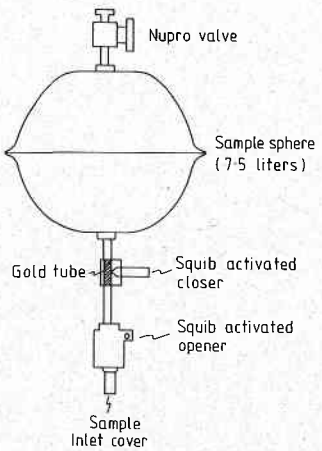

Figure 9 Grab sample sphere assembly

spring-mounted in the spherical gondola. All foam plastics in the other packages were vacuum degassed prior to flight so as to avoid contamination due to outgassing at high altitude (low pressure).

The sampling sequence is initiated after confirmation is received that the balloon has reached its float altitude. The termination command sent at this time also serves to energize the electronic package and the first sample sphere is opened by a squib-activated opener approximately 15 seconds after the parachute descent commences.

A time delay relay then fires a second squib to seal the sphere some 20 seconds later. The remainder of the sequence is controlled by pre-set pressure switches and calibrated time delays.

To accurately maintain the set-point of the pressure switches, the electronics were kept at 20-25°C. Since the pressure/altitude relation was determined during ascent of the main gondola it was easy to determine the average sampling altitude for each sphere. A check of the sampling altitude was also provided by measuring the sphere pressure prior to analyses and of course correcting for the difference in temperature.

It has been shown that air sample integrity for N_2O and the CFMs was preserved with this procedure within the standard deviation of the analyses for at least a one-month period.

Prior to the balloon flight the spheres were prepared as follows: The spheres were attached to an all-metal vacuum manifold inside a large oven, leak-tested and then purged several times with high purity nitrogen. The oven was then heated to ∿200°C and the spheres evacuated for at least 24 hours until the manifold pressure was $<5 \times 10^{-7}$ torr; after cooling, the spheres were exposed to 1,1,1,3,3,3 - hexamethyldisilazane vapours for ∿24 hours; the spheres were then pumped and purged several more times with high purity nitrogen and finally re-pumped to a manifold pressure of $<5 \times 10^{-7}$ torr. The spheres were then sealed for shipment to the launch site.

Following the flight the spheres were returned to the laboratory, the gas pressures determined and the samples transferred to small volume (∿50 cm^3), treated metal tubes (with metal bellows valves) using a liquid helium transfer technique. Prior to the transfer the interconnecting tee-piece was evacuated to $<10^{-5}$ torr.

Tests of the transfer system using small samples of background air showed that the transfer process did not alter the integrity of the sample. Upon completion of the transfer the compression tubes were allowed to sit for approximately 24 hours with differential heating (hot water at one end) to ensure complete re-mixing.

2.5.2 Sample Analyses

Nitrous oxide (N_2O)

Analysis was carried out using a Perkin-Elmer F17 gas chromatograph (GC) fitted with a pulsed electron-capture detector (Ni-63) maintained at 350°C. The 5 ml loop of the gas sample valve was normally flushed with at least 75 cm^3 of sample prior to injection (Roy, 1979). For the two highest samples, only

30-40 cm^3 were used for analysis. Gas separation was achieved with 2.4 m × 3 mm OD columns of Porapak Q and Porapak R with 95% argon/5% methane carrier gas at a flow rate of 25 cm^3/min. The precision of the technique was better than 1%. Gas standards (cryogenically trapped baseline air) were regularly intercalibrated with standards prepared by R.A. Rasmussen (Oregon Graduate Center).

Trichlorofluoromethane (CCl_3F)

The stratospheric air samples were connected directly to the sample loop (5 ml) of a coulometric electron capture detector gas chromatograph (Lovelock, 1974). The detector was fitted with a tritium source (0.4 mCi) and operated in the constant frequency mode. The detector was calibrated using reference gases of compressed ambient air (Fraser, 1980) which, in turn, were calibrated against standards prepared by R.A. Rasmussen. Approximately 20 to 100 ml (at STP) of stratospheric air was used for the analyses, depending on the size of the stratospheric air sample. Both stratospheric air samples and calibration gases were passed through Nafian drier (Foulger and Simmonds, 1979) just prior to the sample loop of the gas chromatograph.

Methane (CH_4)

The methane analysis was conducted on a Hewlett Packard 5730A gas chromatograph with flame ionization detector using a 1 ml sample loop. Reproducibility was ±1% or better. The calibration standard was provided by R.A. Rasmussen.

2.6 Water Vapour

The CSIRO stratospheric water vapour instrument is a radiometer operating in the far infrared (40-200 μ) which measures the emission of radiation by water vapour from two zenith angles (nominally 45° and 70°) by comparison with the emission from an angle at 16° below the horizon. The latter serves as a reference black body emission at ambient temperature. The processed signal is recorded *in situ* on both a Rustrak chart recorder and a cassette tape recorder.

The data is used to compute a parameter Q, where

$$Q = \frac{S_{45} - S_{70}}{S_{45} + S_{70}}$$

where S is proportional to the difference between the below horizon emission and that at either one of the zenith angles. A computation of emissions at these angles from a model stratosphere with a range of assumed water vapour values and temperature characteristics serves as comparison from which the actual water vapour content is deduced. A detailed description of the instrument and method of data reduction may be found in Hyson and Platt (1974) and Hyson (1978). The random errors in the H_2O measurements are ±30% at 15 km rising to ±100% at 27 km.

2.7 Particles

Aerosol concentrations were measured with an *in situ* optical counter which gave the concentration of particles of radius > 0.15 μm and of particles of radius > 0.25 μm. The counter is the same construction as those used extensively by the University of Wyoming atmospheric physics group. The methods of operation and calibration and the analysis techniques have been described by Hofmann et al. (1975).

Each data point includes 500 particles for the small particle measurement and 100 particles for the large particle measurement, giving an uncertainty of ±4% and ±10% respectively in calculated concentration and a separation of data points which is dependent on the concentration but is typically between 300 m and 2 km.

The aerosol data is measured as a function of pressure not elapsed time since launch, so the heights presented in the following tables have been derived from the calculated pressure/height distribution from the radar height and temperature profiles.

3. DATA TABLES

The data from the balloon flights and ground based observations are presented in the following tables. In section 3.1 summary data are presented and then in the following sections more detailed observations are presented where obtained. For HNO_3 and H_2O no detailed information is presented as the data reduction process yields the 1 km interval data presented in the summary tables. The date is presented as a six character number, with the sequence year, month, day. The launch time is presented as a five or six character number with the following sequence, 1 or 2 characters for the hour, 2 characters for the minutes and 2 characters for the seconds. The launch times are in Universal Time, U.T.. All heights are in geometric altitude above mean sea level.

The constituent data, averaged over 1 km intervals centred on the specified altitudes are presented in the following tables. In the top and bottom layers the average data represents that from the nearest half kilometre interval to the height specified (i.e. the heights specified are the maximum balloon height and the height of the launch station respectively. The pressure and temperature data are the point data at the specified altitude (not height averaged). The air total molecular number density is the true average over the height interval. Units are ppbv $\equiv 10^{-9}$ volume mixing ratio, pptv $\equiv 10^{-12}$ volume mixing ratio, ppmm $\equiv 10^{-6}$ mass mixing ratio.

The balloon flight profile and meteorological data give point data collected during the balloon ascent at the specified altitudes. Note the constituent data were often collected on descent and/or ascent so that to know the synchrony between various measurements the detailed data which are presented in a later section must be examined.

These tables, including the ground based total (column density) O_3 and NO_2 data, are presented on the enclosed microfiche.

TABLE CAPTIONS

3.1a Summary of 1 km height averaged constituent data
3.1b Summary of balloon flight profile
3.1c Summary of meteorological data

3.2 Nitric oxide data

3.3 Nitrogen dioxide data

3.4 Radiosonde-ozone sonde data

3.5 Grab sample data

3.6 Particle data

3.7 Total ozone and total nitrogen dioxide data

ACKNOWLEDGEMENTS

This work was performed under Memorandum of Understanding AIA/CA-17 between the Federal Aviation Administration, Department of Transportation, United States of America and the Commonwealth Scientific and Industrial Research Organization Australia. We thank Drs. J. Rogers, N. Sundararaman (FAA), A.B. Pittock, P.J. Fraser and R.N. Kulkarni (CSIRO) for their assistance with this work. Messrs. C. Midwinter, W. Clark (AES), C.M. Elsworth, F.R.E. de Silva, I. Bird, R. McVay, J. Bennett, R. Hill, G. Rutter, N. Bacon (CSIRO) and G.A. Meilak (Melbourne University) along with the Australian Balloon Launching Station staff through their technical assistance in the field programme made these measurements possible. We thank the Bureau of Meteorology, Department of Science and Technology for their generous assistance with forecasts, radar tracking and meteorological data throughout this experiment. Messrs. T. Davies, C. Walley and D. Slater provided other essential help and we thank Mrs. J. Evans for her typing.

REFERENCES

Bass, A.M., A.E. Ledford Jr., A.H. Laufer, 1976: Extinction coefficients of NO_2 and N_2O_4. J.Res. N.B.S., 80A, 143.

Boughner, R., J.C. Larsen, M. Natarajan, 1980: The influence of NO and C&O variations at twilight on the interpretation of solar occultation measurements. Geophys.Res.Lett., 7, 231.

Brewer, A.W., 1973: A replacement for the Dobson spectrophotometer? Pure Appl.Geophys. 106, 919.

Brewer, A.W., C.T. McElroy, J.B. Kerr, 1973: Nitrogen dioxide concentrations in the atmosphere. Nature, 246, 129.

Brewer, A.W., C.T. McElroy, J.B. Kerr, 1974: Spectrophotometric nitrogen dioxide measurements. Proc. CIAP III, U.S. DOT, DOT-TSC-OST-74-15.

Chapman, S., 1931: The absorption and dissociative or ionizing effects of monochromatic radiation in an atmosphere on a rotating earth, 2, grazing incidence. Proc.Phys.Soc. London, 43, 483.

Craig, R.A., 1965: The Upper Atmosphere - Meteorology and Physics. Academic Press.

Dave, J.V., C.L. Mateer, 1967: A preliminary study on the possibility of estimating total atmospheric ozone from satellite measurements. J.Atmos.Sci., 24, 414.

Evans, W.F.J., C.I. Lin, C.L. Midwinter, 1976: The altitude distribution of nitric acid at Churchill. Atmosphere, 14, 172-179.

Fraser, P.J., 1980: Baseline atmospheric halocarbon measurements: an inter-laboratory comparison. WMO Special Environ. Rept. No. 14, 57-63.

Foulger, B.E., P.G. Simmonds, 1979: Drier for field use in the determination of trace atmospheric gases. Anal.Chemistry, 51, 1089-1090.

Goldman, A., T.G. Kyle, F.S. Bonomo, 1971: Statistical band model parameters and integrated intensities for the 5.9 μ, 7.5 μ, and 11.3 μ bands of HNO_3 vapor. Appl.Optics, 10, 65-73.

Goldman, A., F.S. Bonomo, F.P.J. Valero, D. Goorvitch, R.W. Boese, 1981: Temperature dependence of HNO_3 absorption in the 11.3 μm region. Appl.Optics, 20, 172-175.

Hall, T.C., F.E. Blacet, 1952: Separation of the absorption spectra of NO_2 and N_2O_4 in the range 2400-5000 A. J.Chem.Phys., 20, 1745.

Heath, D.F., C.L. Mateer, A.J. Krueger, 1973: The Nimbus backscatter ultraviolet (BUV) atmospheric ozone experiment. Pure Appl.Geophys., 107, 1238.

Hofmann, D.J., J.M. Rosen, T.J. Pefrin, R.G. Pinnick, 1975: Stratospheric aerosol measurements I: Time variations at northern mid-latitudes. J.Atmos.Sci., 32, 1446-1456.

Hudson, R.D., E.I. Reed, 1979: The Stratosphere: Present and Future. NASA Reference Publication 1049, 293.

Hyson, P., C.M.R. Platt, 1974: Radiometric measurements of stratospheric water vapour in the southern hemisphere. J.Geophys.Res., 79, 5001-5005.

Hyson, P., 1978: Stratospheric water vapour measurements over Australia 1973-1976. Quart.J.Roy.Met.Soc., 104, 225-228.

Johnson, H.S., R. Graham, 1981: The absorption cross-sections of NO_2 in the region 417 to 507 nm, private communication.

Kerr, J.B., C.T. McElroy, 1976: Measurement of stratospheric nitrogen dioxide from the A.E.S. Stratospheric Balloon Program. Atmosphere, 14, 166-171.

Kerr, J.B., W.F.J. Evans, J.C. McConnell, 1977: The effects of NO_2 changes at twilight on Tangent Ray NO_2 measurements. Geophys.Res.Lett., 4, 577-579.

Lovelock, J.E., 1974: The electron capture detector, theory and practice. J.Chromatography, 99, 3-12.

Mateer, C.L., 1964: A study of the information content of Umkehr observations. Tech. Report 2, University of Michigan, ORA Project 04682.

Noxon, J.F., E.C. Whipple, Jr. and R.S. Hyde, 1979: Stratospheric NO_2, I. Observational method and behaviour at mid latitude. J.Geophys.Res., 84, 5047-5065.

Pittock, A.B., 1977a: Climatology of the vertical distribution of ozone over Aspendale (38°S 145°E). Quart.J.Roy.Met.Soc., 103, 575-584.

Pittock, A.B., 1977b: Ozone sounding correction procedures and their implications. Quart.J.Roy.Met.Soc., 103, 809-810.

Ridley, B.A., 1978: Measurements of minor constituents of the stratosphere by chemiluminescence. Atmospheric Technology, 9, 27-34.

Ridley, B.A., H.I. Schiff, A. Shaw, L.R. Megill, 1975: In situ measurements of stratospheric nitric oxide using a balloon-borne chemiluminescent instrument. J.Geophys.Res., 80, 1925-1929.

Roy, C.R., 1979: Atmospheric nitrous oxide in the mid-latitudes of the southern hemisphere. J.Geophys.Res., 84, 3711-3718.

Roy, C.R., I.E. Galbally, B.A. Ridley, 1980: Measurements of nitric oxide in the stratosphere of the southern hemisphere. Quart.J.Roy.Met.Soc., 106, 887-894.

Schmeltekopf, A.L., P.D. Goldan, W.R. Henderson, W.J. Harrop, T.L. Thompson, F.C. Fehsenfeld, H.I. Schiff, P.J. Crutzen, I.S.A. Isaksen, E.E. Ferguson, 1975: Measurements of stratospheric $CFCl_3$, CF_2Cl_2 and N_2O, Geophys.Res.Letts., 2, 393.

Seyd, M.Q., Harrison, A.W., 1980: Ground based observations of stratospheric NO_2. Can.J.Phys., 58, 788.

Smith, F.L., C. Smith, 1972: Numerical evaluation of Chapman's grazing incidence integral, $Ch(x,\chi)$. J.Geophys.Res., 77, 3592.

Spillane, K.T., R.R. Brook, 1968: The Laverton Serial Sounding Experiment. Commonwealth of Australia Bureau of Meteorology Report, December, 1968.

APPENDIX

5. ANALYSIS OF PHYSICAL DATA

5.1 General

A meteorological balloon tracking (wind finding) radar was used at Alice Springs and at Mildura, to measure the slant range, azimuth and elevation of the balloon, with respect to the launch site, as a function of elapsed time from launch. Alternatively when the balloon passed out of radar range (160 km) a Raven Tracking Unit was used along with a balloon borne Rosemount pressure probe to provide slant range, azimuth and balloon pressure height.

Detailed balloon flight profile and meteorological data for each flight are presented in the following tables. The balloon ascent rate, wind speed and direction are calculated using the position and height data for the two radar readings adjacent (above and below) the specified height. This effectively smoothes the data, with the ascent rate, wind speed and direction commonly being 8 minute averages on most of the flights. When the balloon passes out of radar range and the pressure height/radio location data are using, the heading description specifies time of commencement of this "Rosemount data" and the flight data sequence is interrupted at the appropriate line specifying "Start of Rosemount/Radio ranging data".

Winds were often not determined during the first few minutes of flight as the exact position of the balloon with respect to the radar on launch was not determined.

The wind speed and direction determined by the radio ranging equipment are very inaccurate as this equipment had a resolution of ±1° in Azimuth and ±1 nautical mile in range.

5.2 Radar measurements

5.2.1 Balloon height

The altitude of the balloon was determined from the radar data via the formula

$$h = ([Re + h_o]^2 + S^2 + 2S\,[Re + h_o]\,\sin\varepsilon)^{1/2} - Re - \frac{(S\cos\varepsilon)^{3/2}}{9200} \quad \ldots (1)$$

where Re = radius of earth

h_o = altitude of launch station

h = altitude of balloon

S = slant range

ε = elevation

The first two terms on the right-hand side of (1) contain the corrections for the curvature of the earth's surface, while the last term is the correction due to atmospheric refraction. At Alice Springs the RMS height error from radar determination is probably 50 metres at maximum range and 30 km altitude, and at Mildura the corresponding error is 200 metres (Spillane and Brook, 1968).

(The last two height determinations on Flight ABLS688 most likely have a larger error than this as the instrument package at this time was rapidly descending by parachute.)

5.2.2 Balloon position

The latitude and longitude of the balloon were determined from the formulae

$$\sin \lambda = \sin \lambda_o \cos \Theta + \cos \lambda_o \sin \Theta \cos A \quad \ldots (2)$$

$$\sin (\phi - \phi_o) = \sin \Theta \sin A / \cos \lambda \quad \ldots (3)$$

$$\text{and } \cos \Theta = ([Re + h_o]^2 + [Re + h]^2 - S^2)/(2[Re + h_o][Re + h]) \quad \ldots (4)$$

where Re, h_o, h, S are as defined before and

λ = latitude of balloon

λ_o = latitude of launch station

ϕ = longitude of balloon

ϕ_o = longitude of launch station

A = true azimuth of balloon from launch station

5.2.3 Solar Zenith Angle

The solar zenith angle Z at any time and balloon position was calculated using the following equations

$$\beta = (279.4574 + 0.985647t) \frac{\pi}{180} \quad \ldots (5)$$

where t = time in days from 00.00.00 hrs U.T., Jan. 1, 1965

$$\tau = t/365.2422 \quad \ldots (6)$$

$$E = (0.033\tau - 429.8) \cos \beta - (102.5 + 0.142\tau) \sin \beta + 596.5 \sin 2\beta - 2 \cos 2\beta + 4.2 \sin 3\beta + 19.3 \cos 3\beta - 12.8 \sin 4\beta \quad \ldots (7)$$

where E is the equation of time in seconds

$$d = \beta - \frac{E}{240} \cdot \frac{\pi}{180} \quad \ldots (8)$$

where d is the right ascension of the sun (in radians)

$$H = \frac{\pi}{720} (t_o + \frac{E}{60} + 720 - 4\phi) \quad \ldots (9)$$

where H = local hour angle (in radians)

t_o = time of day (in minutes)

$$\cos Z = \sin \delta \sin \lambda + \cos \delta \cos \lambda \cos H \qquad \ldots (10)$$

Computations of Z agreed with values derived from a nautical almanac to within 0.05°.

5.2.4 Wind Direction and Speed

The wind direction and wind speed as recorded by the motion of the balloon between times t_1 and t_2 were calculated from the formulae (derived from Craig, 1965)

$$\tan(\Theta - \pi) = \frac{S_2 \cos\varepsilon_2 \sin A_2 - S_1 \cos\varepsilon_1 \sin A_1}{S_2 \cos\varepsilon_2 \cos A_2 - S_1 \cos\varepsilon_1 \cos A_1} \qquad \ldots (11)$$

and

$$v = \frac{50}{3}\left|\frac{S_2 \cos\varepsilon_2 \sin A_2 - S_1 \cos\varepsilon_1 \sin A_1}{(t_2 - t_1)\sin\Theta}\right| \qquad \ldots (12)$$

where Θ = wind direction at time $\frac{1}{2}(t_2+t_1)$

v = wind speed at time $\frac{1}{2}(t_2+t_1)$ in ms^{-1}

S_1, S_2 = slant range in km at time t_1, t_2 in minutes

ε_1 ε_2 = elevation of balloon at time t_1, t_2

A_1, A_2 = reciprocal azimuth of balloon at time t_1, t_2

5.3 Analysis of Rosemount Data

The Rosemount Raven Trak Pack system used for these flights gave readings of pressure, azimuth and slant range as a function of elapsed time.

5.3.1 Balloon Height

The pressure readings were converted to height using the pressure/height relationships derived from the radiosonde carried with each payload (see later).

For those flights for which simultaneous radar and Rosemount data were available the quantity (Rosemount height-radar height) was plotted against radar height. The results are shown in Figure 10. The quantity Rosemount height - radar height varies from -0.6 km to +1.14km, with some indication of systematic as well as random behaviour. Using this plot the Rosemount heights were "corrected" to make the two sets of data more compatible. Other information from a pressure sensor within the nitric oxide detector was used to aid the interpretation of these differences. The corrections applied to the Rosemount data are shown in Table 5.1.

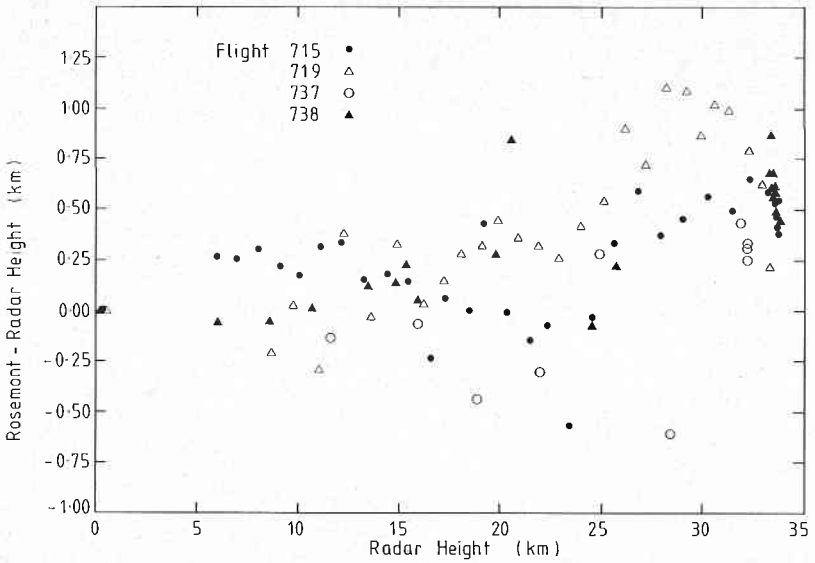

Figure 10 Difference in Rosemount and radar heights as a function of height for ABLS flights 715, 719, 737 and 738

5.3.2 Balloon Position

The latitude and longitude of the balloon were calculated in the same way as for the radar data.

Table 5.1

Corrections (in km) Added to the Measured Rosemount Height

Height Range (km)	Flight No. ABLS 723	ABLS 737	ABLS 738
0-23	-0.11	-0.11	-0.11
23-26	-0.15	-0.15	-0.15
26-35	-0.54	-0.54	-0.54

5.3.3 Wind Direction and Speed

In the absence of any elevation values the wind direction and speed were determined from

$$\tan(\Theta - \pi) = \frac{\Delta\phi\cos\lambda}{\Delta\lambda} \quad \ldots (13)$$

$$v = \frac{50}{3}\left|\frac{R\Delta\phi\cos\lambda}{(t_2-t_1)\sin\Theta}\right| \quad \ldots (14)$$

where R = radius of earth (assumed to be 6371.0 km)

5.4. Analysis of Radiosonde Data

The radiosondes used were Phillips type RS4 MkII.

The sondes, which were flown on both large and small gondolas and independently using meteorological balloons, provided measurements of temperature, pressure and (in the lower atmosphere) humidity as functions of elapsed time from launch. The telemetered data were recorded in real time on a chart recorder.

Most, but not all, of these flights were tracked by radar so the method of data analysis for the pressure/height data was adapted to cope with both possibilities.

5.4.1 Temperature and humidity

The signals corresponding to temperature and/or humidity were read from the chart record at "significant points", i.e. when a change was observed in the linear rate of change of the appropriate signal. The signals were converted to temperature and humidity using the measured calibration factors for the particular sonde being used. At those times when only one of the two quantities was read from the chart record the "missing" signal was calculated by linear interpolation.

The R.M.S. error in the final temperature values was assumed to be 0.7°C (Spillane and Brook, 1968).

5.4.2 Pressure/height

The pressure signal was read from the chart record wherever temperature and/or humidity was read.

For the flights for which radar data was available the altitude was taken to be that derived from the radar data. Given the time at which each sonde measurement was made the corresponding altitude Z was calculated from the radar altitude/time data by linear interpolation. The geopotential altitude was then calculated from the equation

$$\phi = \frac{RZ}{R + Z} \qquad \ldots (1)$$

where ϕ = geopotential altitude

R = radius of earth

Given the pressure p_1, temperature T_1 at geopotential ϕ_1 and temperature T_2 at geopotential ϕ_2 the pressure p_2 was then calculated from

$$p_2 = p_1 \exp \left| - \frac{mg_o}{2R} \frac{T_1 + T_2}{T_1 T_2} (\phi_2 - \phi_1) \right| \qquad \ldots (2)$$

where m = gram-molecular weight of air

g_o = gravitational acceleration at sea-level

The calculation of the pressure profile was started by using the ground-level pressure and temperature values at the launch site.

For those flights for which radar data was not available the pressure values and temperature values were used to deduce the altitude corresponding to each pair of (p, T) values from the formulae

$$\phi_2 = \phi_1 + \frac{R}{2mg_o} (T_1 + T_2) \log_e \left(\frac{p_1}{p_2}\right) \qquad \ldots (3)$$

and

$$Z = \frac{R\phi}{R - \phi} \qquad \ldots (4)$$

where the notation is exactly the same as in (1) and (2).

In this case the solution was started by using the ground-level values of pressure, temperature and geopotential altitude. Comparison of radar and pressure derived heights for nine flights (the latter heights from the radiosonde baroswitch pressure) give a radar-radiosonde height difference of 0.0 ± 0.1 km at 15 km and -0.4 ± 0.7 km at 27 km. It is assumed that the radar heights are more accurate (particularly at lower pressures where temperature and pressure sensor errors amplify the pressure height errors) and radar heights are used whenever available.

The R.M.S. error in baroswitch pressures is typically 1 mb in the interval from the surface to 20 mb (Spillane and Brook, 1968).